

The ZEKE-effect in cold Rydberg gases

S. K. Dutta, D. Feldbaum, G. Raithel

University of Michigan, Physics Department, Ann Arbor, MI 48109-1120

(December 2, 2024)

Cold, dense Rydberg gases produced in a cold-atom trap are investigated using spectroscopic methods and time-resolved electron counting. On the discrete Rydberg resonances we observe large trap losses and long lasting electron emission from the Rydberg gas ($>30\text{ms}$). Our observations are explained by quasi-elastic l -mixing collisions between Rydberg atoms and slow electrons that lead to the population of long-lived high-angular-momentum Rydberg states. These atoms thermally ionize slowly and with large probabilities, leading to the observed effects.

32.80.Pj, 52.25.Ya, 34.60.+z

Laser-cooled atoms can be used to study highly excited Rydberg atoms [1] at both large densities and low atomic velocities. Due to the low velocity of the Rydberg atoms, ionizing Rydberg-Rydberg collisions that dominate the behavior of hot Rydberg gases [2–4] are largely suppressed. Therefore, the interactions between the Rydberg atoms, free electrons and ions result in a variety of novel phenomena that are specific to translationally cold Rydberg gases. Density-dependent effects have been observed in the resonant excitation transfer between cold Rydberg atoms [5,6]. A minute increase of the frequency of the Rydberg excitation laser leads to the production of metastable cold plasmas rather than cold Rydberg gases [7]. At a critical density corresponding to about one atom per atomic volume, Rydberg gases might undergo a Mott transition that would lead to a new kind of metastable matter [8–10]. The formation of metastable Rydberg matter might proceed through an intermediate phase, in which the Rydberg population accumulates in long-lived high-angular-momentum (high- l) states [10]. In the present paper, we show that in cold Rydberg gases high- l Rydberg states are efficiently produced by a robust mechanism, which is, in a similar form, also at work in ZEKE (ZEro Kinetic Energy) electron - spectroscopy, a powerful technique that has revolutionized molecular spectroscopy [11].

In our experimental cycle, ^{87}Rb atoms are collected and cooled in a magneto-optic trap (MOT [12], see Fig. 1) for about 950ms. 1ms after the shutdown of the MOT a $5\mu\text{s}$ long diode laser pulse ($\lambda = 780\text{nm}$) resonant with the $5S_{1/2}, F = 2 \rightarrow 5P_{3/2}, F = 3$ transition is applied. While the 780nm pulse is on, a blue dye laser pulse ($\lambda \approx 480\text{nm}$, 10ns width, bandwidth $\approx 15\text{GHz}$, repetition rate 10Hz) excites ns - and nd -Rydberg states from the intermediate $5P_{3/2}$ -level. The maximum photon fluence of one blue

pulse easily exceeds the saturation fluence at the photoionization threshold ($7 \times 10^{16}\text{cm}^{-2}$ at $\lambda_{\text{ion}} = 479.1\text{nm}$ [13]). If the dye laser operates with the oscillator only, the broad-band ASE (amplified spontaneous emission) contained in the blue pulse is $< 1\%$ of the pulse energy ($\approx 50\mu\text{J}$). With the dye amplifiers on, the ASE contains $\approx 10\%$ of the pulse energy, is about 5nm wide and centered at $\lambda = 478\text{nm}$, which is above the ionization threshold. The pulsed dye laser is pumped by the 3rd harmonic of a Nd-YAG laser (355nm), a small fraction of which ($< 1\text{mJ}$) can be diverted to partially ionize the atomic cloud before the blue laser pulse arrives. The Rydberg excitation causes a reduction of the ground-state population, which reduces the area density of ground-state atoms that we measure with a low-intensity probe laser pulse resonant on the $5S_{1/2}, F = 2 \rightarrow 5P_{3/2}, F = 3$ transition. A microchannel-plate (MCP) detector located about 10cm from the atomic cloud is used to detect electrons emitted from the Rydberg gas.

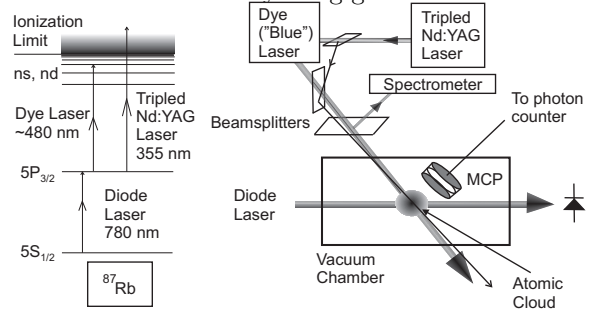


FIG. 1. Level scheme (left) and outline of the experimental setup (right).

Fig. 2a) shows a trap-loss spectrum taken with both the $5S_{1/2} \rightarrow 5P_{3/2}$ and the Rydberg transition saturated. In the continuum as well as on the discrete Rydberg resonances up to about 70% of the atoms are removed. The trap-loss spectra are largely independent of the time at which the probe pulse is applied. Thus, the observed trap loss is mostly due to the *permanent* loss of atoms from the trap upon excitation. The observed trap loss is a cumulative effect, as each trapped atom experiences many blue laser pulses during the MOT loading time (2.5s). We have used a simple model of the MOT loading dynamics to estimate the single-pulse loss fraction X . In Fig. 2b), a floor of $X \approx 1\%$ is observed between the discrete Rydberg lines, which is due to direct photoionization by the above discussed 10% ASE of the blue pulse. The discrete Rydberg lines peak at an X of up to 8% above the floor, a value that corresponds to one-third loss of the excited

Rydberg atom population. Further, there is no significant change in X at the continuum threshold. Our observations show that there is a process by which initially bound Rydberg atoms permanently leave the trap with an efficiency that rivals direct optical photoionization.

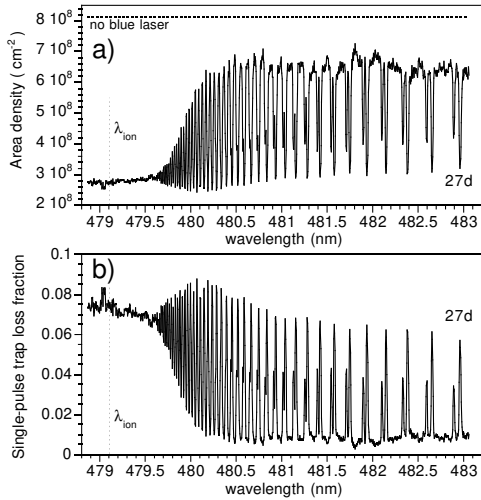


FIG. 2. Rydberg excitation spectrum of atoms in a magneto-optic trap. Panel a): central area density of trapped atoms vs. the wavelength of the blue laser. Panel b): Corresponding estimated single-pulse loss fraction X .

Two-body ionizing Rydberg-Rydberg collisions could, in principle, cause a trap loss. Based on an ionization cross section given in [4], a Rydberg atom velocity of 0.1 m/s, a lifetime of $100\mu\text{s}$ ($n \approx 40$), and a Rydberg atom density of $5 \times 10^9 \text{ cm}^{-3}$ we estimate a collisional ionization probability of $\approx 0.5\%$ of the excited Rydberg population, corresponding to an $X \approx 0.13\%$. This figure is too small for two-body ionizing Rydberg-Rydberg collisions to be the dominant source of trap loss.

To estimate the importance of thermally induced microwave ionization of the excited ns and nd Rydberg states, we have performed rate equation simulations of the population flow among the bound atomic states and the continuum. We use a basis (n, l) of discrete levels up to $n = 100$ with all allowed values of l and the proper quantum defects, and a grid of 10100 continuum states (ϵ, l) with energies up to $\epsilon = 130 \text{ meV}$ and $l = 0, 1, \dots, 101$. Due to isotropy, we can assume uniform distributions over the magnetic substates and use m -averaged transition rates [1]. The obtained thermal ionization probabilities for an ideal 300K blackbody spectrum are displayed in Fig. 3.

While direct thermal ionization of the initially excited states does not cause enough ionization to explain the observed trap loss - see Fig. 3 -, it produces ions moving at about 1 m/s and electrons with about 8 meV average kinetic energy; the latter figure results from the rate-equation calculations. Based on Fig. 3 and on the number of excited Rydberg atoms, we estimate that up

to $\sim 10^5$ electron-ion pairs are created. If the blue laser is used with its amplifiers active, the ionizing ASE of the blue laser pulse adds a significant amount of additional electron-ion pairs (electron energy $\approx 10 \text{ meV}$). As a result, conditions are such that a metastable cold plasma is formed [7]: A fraction of the electrons quickly evaporates, leaving behind a plasma with a net positive charge that acts as an electron trap. If, under our conditions, the initial number of electrons exceeds about 1000, the trap becomes deep enough to retain a fraction of the electrons [7]. The net positive charge causes a slow Coulomb expansion, due to which all trapped electrons eventually evaporate. The electron storage time is thereby limited to of order $100\mu\text{s}$, which is long enough for the retained electrons to frequently collide with the main product of the laser excitation - the bound Rydberg atoms floating in the plasma. The collisions initiate a sequence of events we refer to as the ZEKE-effect.

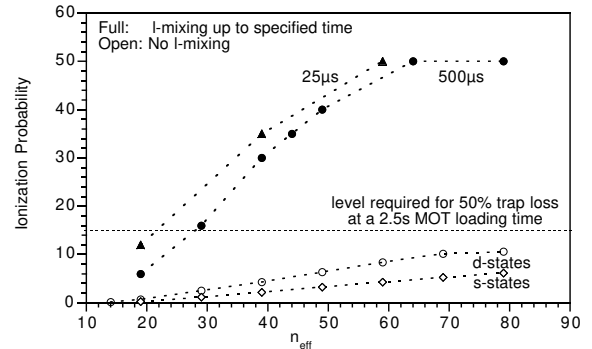


FIG. 3. Thermal ionization probabilities of Rydberg atoms vs. the effective principal quantum number obtained from rate-equation calculations. Open circles: nd -states, open diamonds: ns -states, full circles: l -mixing for $t < 500\mu\text{s}$, full boxes: l -mixing for $t < 25\mu\text{s}$. The curves are explained in the text.

In step A of the ZEKE-effect (see Fig. 4), the atoms are promoted from their initial s or d -states into a high- l -state by the electric-field sweep produced by a bypassing electron. The field sweep brings the initial Rydberg state in contact with a hydrogenic manifold of high- l states, and state-mixing causes a quasi-elastic transition of the atom into a superposition of high- l -states. To model these collisions, we have numerically solved the time-dependent Schrödinger equation. For a given initial state $|n_0, l_0, m_0\rangle$, electron velocity v and collision parameter b the calculation yields a final probability $P(n_0, l_0, v, b)$ of finding the atom in the hydrogenic manifold, i.e. in a state with $l \geq 4$. For $l_0 \neq 0$, we run the calculation for the allowed values of m_0 and average the resultant probabilities over m_0 . The cross section σ for a transition into $l \geq 4$ is then defined as

$$\sigma(n_0, l_0, v) = \int_{b=0}^{b=\infty} P(n_0, l_0, v, b) 2\pi b db \quad (1)$$

For $l_0 = 0, 1$ or 2 it is easy to determine an upper cutoff value for b where $P \rightarrow 0$. The range $b < a_0 n^2$, where the neglected ionizing processes should become dominating [4], does not significantly contribute to σ .

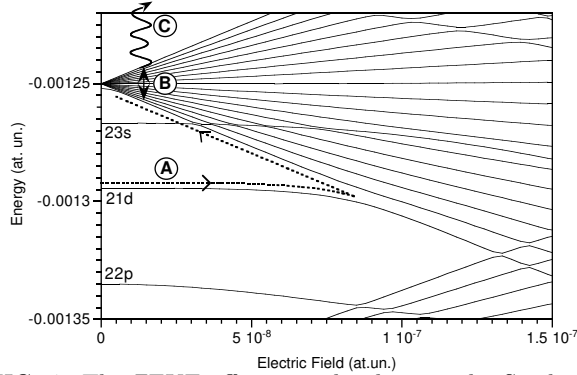


FIG. 4. The ZEKE effect visualized using the Stark map of Rb in the vicinity of $n = 20$. The three steps A, B and C, explained in the text, lead to the production of long-lived Rydberg atoms and time-delayed thermal ionization. The step A is induced by quasi-elastic collisions between electrons and Rydberg atoms.

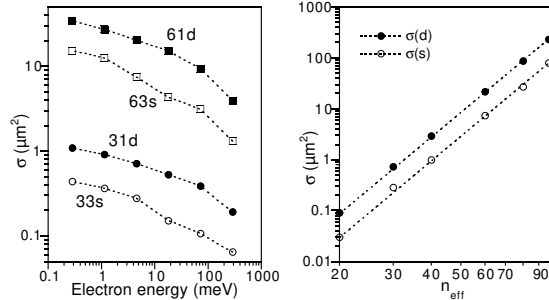


FIG. 5. Left: Calculated l -mixing cross sections σ for collisions of Rydberg atoms in the indicated initial states with electrons versus the electron energy. Right: l -mixing cross sections σ with n_{eff}^5 -fits (dotted) for s - and d -initial states at an electron energy of 4.5meV versus the effective quantum number.

Fig. 5 shows the results of our cross section calculations for the s and d -states of two values of n . The drop of σ at higher electron energy reflects the fact that the passage behavior of the Rydberg atoms in the Stark map (Fig. 4) turns diabatic. The s -states generally have cross sections about 2.5 times smaller than the cross sections of the nearest d -state. This reflects the diabatic crossing behavior of the s -state atoms with the lowest few states of the nearest hydrogenic manifold - note the narrow anticrossings in Fig. 4. For fixed electron energy, the cross sections approximately scale as n_{eff}^5 . The average values of l of the atoms that made a transition into the hydrogenic manifold are of order $n/2$ (not shown), i.e. the l -distribution becomes pretty well randomized within the hydrogenic manifold.

The plasma volume ($\approx 1\text{mm}^{-3}$), the electron number (≥ 1000), the electron velocity ($\approx 50000\text{ m/s}$), the electron storage time ($\approx 100\mu\text{s}$), and the cross sections depicted in Fig. 5 lead to the conclusion that the step A in Fig. 4 happens with certainty for n larger than about 20. The presence of the plasma that temporarily traps the electrons is crucial, as it keeps the electrons from leaving and causes them to frequently collide with the abundant, bound Rydberg atoms floating in the plasma. Collisions between Rydberg atoms and ions are ineffective, because the ions are very slow ($\approx 1\text{m/s}$), as are the Rydberg atoms themselves.

After step A in Fig. 4, the weak but rapidly varying microfields generated by more distant electrons will be sufficient to further randomize the Rydberg population among the quantum-defect-free hydrogenic states (step B). Step B is more probable than step A, but it is not required for the subsequent step C. Once all plasma electrons have evaporated, the only electric fields the Rydberg atoms are still exposed to are the fields generated by the very slowly moving ions. Therefore, we expect that the plasma dynamics and the internal dynamics of the Rydberg atoms decouple at about $100\mu\text{s}$ after the excitation.

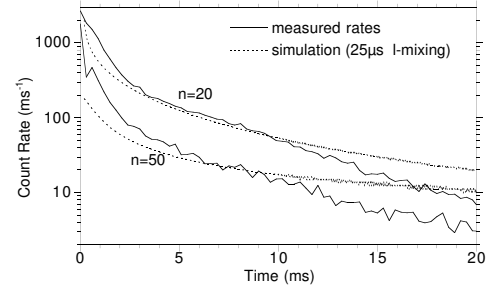


FIG. 6. Electron count rates for the indicated Rydberg d -states vs. the delay time between the Rydberg excitation and the counting gate. The signal lasts at least 100 times as long as the natural lifetime of the initially excited states, and shares the qualitative features of simulated results (dotted).

Subsequently, while the cloud of high- l Rydberg atoms produced by the steps A and B slowly expands, the atoms decay or thermally ionize on a slow time scale (step C in Fig. 4). To model the overall dynamics of the Rydberg population, we have included an initial “plasma phase” in our rate-equation simulations. During that phase, the populations in the n -manifolds and the nearby non-hydrogenic states are periodically averaged over the allowed l -values (with weights $\sim (2l+1)$); after the “plasma phase” the averaging ceases. The obtained ionization probabilities are displayed in Fig. 3 for $25\mu\text{s}$ and $500\mu\text{s}$ long plasma phases. The ionization probabilities are stable against variations of the duration of the plasma phase and are large enough to explain the experimentally observed trap losses.

The discussed model is supported by the results de-

scribed in the following. Using the MCP detector located near the atom trap, we have measured the thermal ionization current vs. time (Fig. 6). When we excite discrete Rydberg levels, we find long-lived electron signals that extend beyond 30ms and that only occur if the frequency of the blue laser is resonant with a discrete Rydberg line. The delayed electron signal, which is characteristic for the ZEKE-effect [11], is due to thermal ionization of high- l Rydberg states.

Fig. 7 shows the electron current in a time-delayed counting window vs. the wavelength of the blue laser for conditions well below the saturation of the Rydberg transition. The clarity of the ionization threshold in the long-lived electron signal, which is typical for the ZEKE-effect [11], shows that the delayed electrons are linked to the initial optical excitation of bound Rydberg atoms. In Fig. 7a) the blue pulse is generated with the dye laser oscillator only, which has practically no ASE. Therefore, all electron-ion pairs that are created within about $100\mu\text{s}$ from the Rydberg excitation originate in thermal ionization of the excited ns - or nd -Rydberg atoms. Since the $5P \rightarrow ns$ -photoexcitation cross sections are about six times smaller than the ones of the neighboring d -states, and since the thermal ionization probability of the s -states is only half that of the neighboring d -states (see Fig. 3), the thermal electron yield on the s -lines is less than one-tenth of the yield on the neighboring d -lines. Recalling that of order 1000 slow electrons are needed to form the essential cold-plasma electron trap - with some electrons left in it -, it follows that there is a wide range of parameters where the ZEKE-signal should occur on the d -lines, but not on the neighboring s -lines. Fig. 7a), where the s -lines barely appear, shows one such case.

We have used two methods to force a ZEKE-signal on the s -lines in cases where it would normally not appear. In Fig. 7b) we have used the same parameters as in a), except that the blue laser pulse has been generated with a dye-laser amplifier being active. The pulse has then been attenuated to the same pulse energy as in a). The ASE produced by the amplifier creates enough slow electron-ion pairs to form the cold-plasma electron trap, independent of whether the coherent part of the laser excites d or s Rydberg atoms. As a result, we observe both s and d lines in the ZEKE-signal. In Fig. 7c), the blue laser pulse is the same as in a), i.e. it has no ASE, but we ionize a small fraction of the atoms by a UV laser pulse that hits the cloud a few ns before the blue laser pulse (see Fig. 1). The electrons produced by the UV pulse have an energy of about 1eV and therefore all leave. The remaining electron-free potential well captures any slow electrons that are subsequently produced. The comparatively few thermal electrons produced on the s -lines now don't escape, as in the case of Fig. 7 a), but are trapped and trigger the ZEKE-effect (note the s -lines in Fig. 7c)).

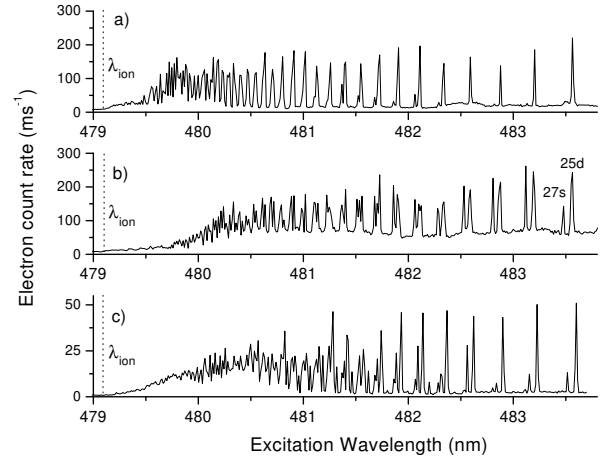


FIG. 7. Electron current emitted by the Rydberg gas in a time window from 5ms to 6ms after the excitation as a function of the wavelength of the blue laser. a) $< 1\%$ ASE in the laser spectrum. b) $\approx 10\%$ ASE in the laser spectrum. c) as a), but a weak UV pulse is used to ionize about 0.1% of the atoms a few ns before the blue laser pulse.

In this paper we have shown that dense, cold Rydberg gases in a room-temperature thermal radiation field decay via the ZEKE-effect, which involves the quasi-elastic collisional production of high- l Rydberg states and unusually slow thermal ionization. The effect hinges on the temporary existence of a cold plasma, which acts as a transient electron trap. The stability of the observed phenomenon makes it likely that it represents the generic decay pattern of cold, dense Rydberg gases. It appears likely that the spontaneous and efficient production of high- l Rydberg states could aid the formation of condensed Rydberg matter [9,10]. Since it has become apparent that the radiation temperature is one of the most important parameters of the system, we intend to perform future studies in a cryogenic enclosure with variable wall temperature.

We thank Prof. P. Bucksbaum for inspiring discussions and generous loaning of equipment. Support by NSF and DoE is acknowledged.

-
- [1] T. F. Gallagher, *Rydberg Atoms*, Cambridge University Press, Cambridge 1994.
 - [2] M. Ciocca *et al.*, Phys. Rev. Lett. **56**, 704 (1986).
 - [3] M. W. McGeoch, R. E. Schlier, G. K. Chawla, Phys. Rev. Lett. **61**, 2088 (1988).
 - [4] G. Vitrant, J. M. Raimond, M. Gross, S. Haroche, J. Phys. **B 15**, L49 (1982).
 - [5] W. R. Anderson, J. R. Veale, T. F. Gallagher, Phys. Rev. Lett. **80**, 249 (1998).

- [6] I. Mourachko *et al.* Phys. Rev. Lett. **80**, 253 (1998).
- [7] T. C. Killian *et. al.*, Phys. Rev. Lett. **83**, 4776 (1999)
- [8] N. F. Mott, Proc. R. Soc. London **A382**, 1 (1982)
- [9] E. A. Manykin, M. I. Ozhovan, P. P. Poluektov, Sov. Phys. JETP **57**, 256 (1983), L. Homlid, E. A. Manykin, Zh. Eksp. Theor. Fiz. **111**, 1601 (1997).
- [10] R. Svensson, L. Holmlid, L. Lundgren, J. Appl. Phys. **70**, 1489 (1991), E. R. Olsson, R. Svensson, J. Davidsson, J. Phys. **D 28**, 479 (1995), R. Svensson, L. Holmlid, Phys. Rev. Lett. **83**, 1739 (1999).
- [11] the field is reviewed by E. W. Schlag, R. D. Levine, Comm. At. Mol. Phys. **33**, 159 (1997). The importance of collisions has been stressed by W. A. Chupka, J. Chem. Phys. **99**, 4580 (1993) and P. Bellomo, D. Farelly, T. Uzer, J. Chem. Phys. **108**, 5259 (1998).
- [12] E. L. Raab, M. G. Prentiss, A. E. Cable, A. Clairon, S. Chu, D. E. Pritchard, Phys. Rev. Lett. **59**, 2631 (1987).
- [13] C. Gabbanini *et. al.*, J. Phys. **B 31**, 4143 (1998).